NASA TECHNICAL MEMORANDUM

NASA TM X-52914

NASA TM X-52914

PAIRED COMPARISON TESTS OF THE RELATIVE SIGNAL DETECTED BY CAPACITIVE AND FLOATING LANGMUIR PROBES IN TURBULENT PLASMA FROM 0.2 TO 10 MHz

by J. Reece Roth and Walter M. Krawczonek
Lewis Research Center
Cleveland, Ohio

TECHNICAL PAPER prepared for presentation at Twelfth Annual Meeting of the Division of Plasma Physics of the American Physical Society
Washington, D.C., November 4-7, 1970

E-6011

PAIRED COMPARISON TESTS OF THE RELATIVE SIGNAL DETECTED BY CAPACITIVE AND FLOATING LANGMUIR PROBES IN TURBULENT PLASMA FROM 0.2 to 10 MHz

by J. Reece Roth and Walter M. Krawczonek

National Aeronautics and Space Administration
Lewis Research Center
Cleveland, Ohio

ABSTRACT

Paired comparison measurements of the spectrum of electrostatic potential fluctuations in a steady-state, turbulent plasma confined in a magnetic mirror geometry have been made with capacitive and floating Langmuir probes over the frequency range from 0.2 to 10.0 MHz. For the experimental conditions investigated ($5\times10^7 \leq n_e \leq 5\times10^8/cm^3$, $8 \leq T_e \leq 38$ eV, $350 \leq T_i \leq 930$ eV, $B_{max} = 1.0T$), no significant difference in the relative frequency response was observed below 4.0 MHz. At about this frequency, however, the signal detected by the floating Langmuir probe dropped off relative to that of the capacitive probe. The source resistance of the turbulent fluctuations sensed by the Langmuir probe was about 400 ohms. At higher frequencies, from 7.0 to 10.0 MHz, a signal was detected by the floating Langmuir probe that was not detected by the capacitive probe. This "spurious" signal may be confused with the turbulent fluctuations of the plasma in the absence of paired comparison tests.

INTRODUCTION

In the last decade, the Langmuir probe has been increasingly used by investigators of plasma turbulence to measure fluctuations of such plasma-related parameters as ion saturation current[1-5] and floating potential.[5-8] Most turbulence theories are expressed in terms of electric field strength, electrostatic potential, or charged particle number density fluctuation spectra. The use of Langmuir probes to obtain data for comparison with these theories requires several assumptions.

The first assumption, required when using biased Langmuir probes, is that the saturation current fluctuations are linearly related to the fluctuations of either the charge density, the electric field, or the electrostatic potential. The most common assumption is that the ion saturation current fluctuations are proportional to the fluctuations in charge density. Such a relation implies, among other things, that the electron kinetic temperature is constant in time. A second assumption is that the effective source resistance of the fluctuations is low, such that the probe-plasma sheath does not attenuate, as a function of frequency, the fluctuations that would exist in the absence of the probe. A third assumption is that the probe introduces no spurious noise due to processes in the sheath or on the probe surface. One may circumvent the first assumption by studying only the potential fluctuations with a floating Langmuir probe. The last two assumptions, however, still remain.

The validity of the first assumption has been investigated[9-13] and it has been found that one cannot, in general, assume a linear proportionality between the amplitude of ion saturation current fluctuations and either density or potential fluctuations, without taking into account fluctuations in other plasma properties. With respect to the second and third assumptions, Serafini[4,5] has shown that the background turbulence spectra obtained with floating and positively biased Langmuir probes have the same proportional dependence on frequency above a few hundred kHz. In later work, however, Serafini[8] showed that the frequency spectrum of a Langmuir probe operating at ion saturation differed substantially from that observed with a capacitive probe, at frequencies above 1.0 MHz. There have been isolated indications in the recent literature that the third assumption discussed above may not be valid. Malmberg et al.[14] have observed spurious signals over a frequency range of 50 to 150 MHz that apparently arise in the Langmuir probe sheath. Schmidt[15] and Lencioni et al.[16] report Langmuir probe generated oscillations in a toroidal octupole at frequencies of about 100 kHz.

The objective of the present investigation is to systematically test the validity of the second and third assumptions discussed above for a floating Langmuir probe. This has been done by paired comparisons in a plasma of the Langmuir probe, over frequencies from 0.2 to 10 MHz, relative to that of the capacitive probe described by Schmidt.[15] The capacitive probe was taken as a standard of comparison. These paired comparison tests in a plasma provide information about the plasma-probe interaction that cannot be obtained from conventional workbench calibrations. The range of plasma characteristics covered by this investigation is listed in Table I. Where the frequency spectra of floating potential agree for the two probes, one may presumably use either with confidence for such measurements. Where they do not agree, the second or third assumption discussed above are presumably not valid, and the capacitive probe is then the instrument of choice for the measurement of the spectrum of electrostatic potential fluctuations.

EQUIVALENT CIRCUITS OF PROBES

On Fig. 1 is shown a cross-sectional drawing of the two probes used in the present investigation. The shielded Langmuir probe shown in Fig. 1(a) is of conventional design, with 4 mm of 0.025-mm diameter tungsten wire projecting from a quartz insulating sleeve. The probe wire is surrounded by a coaxial grounded shield within the body of the probe, starting 6 mm from the probe tip. Some supplementary paired comparison runs were taken with an unshielded Langmuir probe, in which the probe wire was covered with a quartz sleeve to within 4 mm of the tip, and the coaxial metal shield did not begin until a distance of 44 mm from the probe tip.

The capacitive probe shown on Fig. 1(b) is similar to that described by Schmidt.[15] The capacitor plate within the probe tip is surrounded by a ceramic envelope, and its lead wire is surrounded by a grounded coaxial shield which begins 6 mm from the tip. Paired comparison tests were also conducted with a capacitive probe identical with that shown, but with a pyrex envelope replacing the ceramic envelope over the probe tip.

The equivalent electrical circuit for the floating Langmuir probe in a plasma is shown in Fig. 2(a). The resistance R_s includes the effects of both the ambient plasma and the sheath, and is assumed real and independent of frequency. The capacitances C_1 and C_2 are, respectively, that of the probe and of the coaxial cable which connects the probe to the external circuit. The frequency response of this circuit is given by

$$e_o = \frac{1}{1 + j\omega CR_s} \tag{1}$$

for the signal which is detected at the cathode follower. In this expression, R_s is the effective source resistance of the plasma fluctuations, and $C = C_1 + C_2$.

The equivalent electrical circuit of the capacitive probe is shown in Fig. 2(b). The resistance R_s includes the effects of the plasma and sheath. The capacitances C_1 and C_2 have the same significance as they did with the Langmuir probe. The frequency response of the capacitive probe equivalent circuit shown in Fig. 2(b) is

$$e_o = \frac{1}{1 + j\omega CR_s + C/C_3} = \frac{1}{266 + j\omega CR_s} \tag{2}$$

for the signal detected by the external circuit. Here again $C = C_1 + C_2$. The capacitances have been measured, and for the probe design and circuitry used in this investigation were typically found to be $C = 106$ pF and $C_3 = 0.4$ pF for the capacitive probe, and $C = 112$ pF for the Langmuir probe. The low frequency cut-off is determined by the input impedance of the cathode followers. The attenuation of the capacitive probe is given by

$$A = (C_1 + C_2 + C_3)/C_3$$

and is 266 for the capacitive probe just discussed. Typical circuit parameters for the capacitive and Langmuir probes used in this investigation are listed in Table II. The difference in the capacitance C_1 of the shielded and unshielded Langmuir probes was approximately 8 pF. The sample-to-sample variation of the probe capacitances was no more than ± 10 percent in this investigation. On Fig. 3 is plotted the theoretical frequency response, from Eqs. (1) and (2), for the parameters shown in Table II and for several source resistances. The solid line is the response curve for the shielded Langmuir probe, and the dotted line is the response curve of the capacitive probe. For a given value of R_s, the capacitive probe will roll off at higher frequencies than the Langmuir probe. It was for this reason that the capacitive probe was chosen as a standard of comparison.

PROBE INSTRUMENTATION

On Fig. 4 is a block diagram of the probe instrumentation used in this investigation. The experimental apparatus necessitated a 166-cm long separation between the probes and the cathode followers. The cathode followers shown had a nominal input impedance of 40 megohms shunted by 4 pF. The Tektronix 1A5 amplifier had an essentially flat frequency response up to 15 MHz, and was not used in the differential mode for this investigation. The output of the amplifier was fed into one of two spectrum analyzers, which covered the ranges 0-1 MHz and 1-10 MHz.

On Fig. 5 is shown a drawing of the forked probe mount located in the calibration cup. The inner plate of this cup was fed with a constant amplitude sinusoidal signal from a variable frequency oscillator which spanned the range 100 Hz to 10 MHz. The provisions for grounding the probe mount and the associated circuitry were refined until a flat frequency response was obtained, free of resonances and absorption. Fig. 6 is the in situ calibration of both probes in the vacuum tank, with all components of the measuring system shown on Fig. 4 except the high-pass filter. In the in situ calibration, the frequency response of both the capacitive and Langmuir probes was essentially flat over the range of interest. Any relative roll-off of the Langmuir probe could therefore be ascribed to the effects of the probe-plasma interaction.

The frequency response of the entire probe system was measured before and after each series of runs by injecting a constant amplitude signal on the inner plate of the calibration cup for twenty frequencies spanning the range of each spectrum analyzer. Unless otherwise noted, all fluctuation spectra plotted below on log-log scales have been corrected for the nonlinearities of the spectrum analyzers and of the recording system.

EXPERIMENTAL APPARATUS

The superconducting magnet facility in which this experiment was conducted has been described elsewhere.[17] It consists of a pair of 18-cm ID superconducting coils shown on Fig. 7, with an inside diameter of 17 cm in a magnetic bottle configuration. The maximum magnetic field strength on the axis occurred at the magnetic mirrors and was 1.0 T for this experiment. The coils were arranged with a mirror ratio

$B_{min}/B_{max} = 0.38$. The steady-state, modified Penning discharge[18] was used in the present series of experiments to produce a hot-ion plasma, the range of parameters of which are shown in Table I.

A cut-away top view of the vacuum tank is shown in Fig. 7. The forked probe mount used to compare the probes in question was positioned so that a 180-degree rotation about its axis would interchange the two probe tips so that they could alternately sample the same volume of plasma. It is estimated that the probe tips, after rotation by 180 degrees, were within the same cubical volume 2 mm on a side. Each probe was 2.48 cm from the magnetic axis of the plasma, and parallel to it. The axial position of the probes was chosen at the position of maximum axial magnetic field gradient, 9.4 cm from the midplane. The magnetic field at the probe tips was 0.65 T, the radial magnetic field gradient 2.35 T/m, and the axial magnetic field gradient 6.0 T/m. These magnetic fields and magnetic field gradients are uncertain by 5 percent. The absolute value of the peak-to-peak oscillations in potential were on the order of hundreds of volts at the probe tip.

The kinetic temperature and relative number density of the ions escaping through the magnetic mirrors were measured by a retarding potential energy analyzer.[19] Precautions were taken to maintain the plasma properties constant during the course of a paired comparison run. Absolute values of the electron number density and kinetic temperature were measured by taking conventional Langmuir probe traces at the location within the plasma at which the paired comparison tests were performed.

The plasma as a whole was a strong r. f. radiator in the range investigated. Some of this radiation was picked up by the instrumentation and contributed to the system background noise in spite of shielding precautions. The total system noise was determined by grounding the input to the 1A5 amplifier. This noise was subtracted from the total signal detected by the probe at a given frequency. The probe signal became comparable to the system noise only at the lowest turbulent amplitudes and/or plasma energy densities investigated.

PAIRED COMPARISON TESTS

The operating conditions were fixed at the beginning of each experimental run, and the plasma allowed to stabilize for at least 5 minutes before data were taken. When the plasma stabilized, a retarding-potential curve was taken to determine the ion energy. Turbulence spectra were taken from both probes. Typical spectra from both probes are shown in Fig. 8 for the frequency range 0.2 to 10 MHz. These data were tabulated, corrected for the nonlinearities in the observing system, and converted to a logarithmic base. The ratio of the corrected data for both probes shown in Fig. 8 is plotted in Fig. 9. The relative frequency response of both probes was the same within experimental error below about 4 MHz. This result held true for all plasma conditions studied. The flatness of the relative frequency response of the shielded Langmuir probe out of this frequency implies that the effective source resistance of the plasma fluctuations is equivalent to a pure resistance of no more than about 400 ohms. The ion cyclotron resonance frequency at the probe tip was 5 MHz in the present experiment. Under the conditions studied a dip in the turbulence spectrum, such as that reported by Batten et al.[1] was not observed at this frequency.

A total of 44 paired comparisons were made of the shielded Langmuir probe with the ceramic covered capacitive probe in the present investigation. The spectra from these runs were classified into one of the four categories illustrated schematically in Fig. 10, or into a fifth category which included all other types of relative frequency response. Figure 10(a) illustrates the situation in which the Langmuir probe signal falls off relative to the capacitive probe, but no noise is observed from the former near the upper frequency limit. Data of this type were observed at intermediate or low turbulent amplitudes and/or plasma energy densities. 45.5 percent of the runs were of this type. Figure 10(b) illustrates the relative fall-off of the Langmuir probe signal, but with a "spurious" signal detected by it at higher frequencies. 34 percent of the runs were of this type, and were observed at intermediate or high turbulent amplitudes and/or plasma energy densities in the range studied. Figure 10(c) illustrates the situation in which the Langmuir probe trace disappeared into the system noise before the relative fall-off could be observed, but the "spurious" signal at high frequencies was above the noise. 4.6 percent of the runs were of this type, and were observed at intermediate turbulent amplitudes and/or plasma energy densities in the range studied. Figure 10(d) is the case in which the spectrum of one or both probes disappeared in the system noise below a frequency of 10 MHz, and neither the relative fall-off nor the noise at higher frequencies could be observed. 13.6 percent of the runs were of this type, and were observed at the lowest turbulent amplitudes and/or plasma energy densities in the range studied. The spectra shown schematically in Fig. 10 are without oscillation peaks, although the simultaneous appearance of such peaks in both spectra were often observed. The absolute number and percentage of the 44 paired comparisons that fell into these categories is shown in Table III. When either the relative fall-off or the spurious noise pick-up of the Langmuir probe was not observed, this may well have been because they were below the system noise threshold, and masked by it. There were no clear-cut cases observed in which the probe signal was well above the noise, and these features were absent.

A total of 13 additional runs were made comparing the ceramic with the pyrex covered capacitive probes. The relative response of these two types of probes was identical within experimental error over the frequency range studied. The ceramic covered capacitive probe was compared with an unshielded Langmuir probe. A total of 16 runs showed essentially the same behavior as that observed with the shielded Langmuir probe comparisons. A total of 17 runs were taken to compare the shielded and unshielded Langmuir probe response. The relative response of these two probes was essentially the same, except for a higher spurious noise signal for the unshielded Langmuir probe at frequencies from 7 to 10 MHz.

CONCLUSIONS

The paired comparison runs performed in this study appear to justify the following conclusions:

1. Over the range of plasma parameters covered in this study, and listed in Table I, the relative frequency response of capacitive and floating, shielded Langmuir probes is the same to within ±20 percent up to about 4 MHz.

2. For the conditions investigated, the response of the floating, shielded Langmuir probe falls off relative to that of the capacitive probe at about 4 MHz.

3. For the plasma conditions investigated, the floating, shielded Langmuir probe detected substantially more signal between 7 to 10 MHz than did the capacitive probe. This "spurious" signal could not be related to any natural frequency of oscillation of the plasma listed in Table I, and may be associated with processes in the sheath surrounding the Langmuir probe tip that are not prevalent in the sheath surrounding the capacitive probe.

4. Over the range of conditions investigated, the relative response of capacitive probes with a pyrex and ceramic envelope were identical within the experimental error.

5. Over the range of plasma conditions investigated, the relative response of the floating shielded and unshielded Langmuir probes were the same, except for the greater signal amplitude, from 7 to 10 MHz, of the unshielded probe.

6. A dip in the spectrum at the ion cyclotron frequency, reported by Batten et al.,[1] was not observed in the present investigation.

7. In terms of physical ruggedness and frequency response in the workbench calibration apparatus, the capacitive probe is superior to the floating, shielded Langmuir probe for measurement of the spectrum of electrostatic potential fluctuations in a plasma.

REFERENCES

1. H. W. Batten, H. L. Smith, and H. C. Early, J. Franklin Inst. 262, 17 (1956).
2. K. Bol, Phys. Fluids 7, 1855 (1964).
3. F. F. Chen, Phys. Rev. Letters 15, 381 (1965).
4. J. S. Serafini, Bull. Am. Phys. Soc. 13, 278 (1968).
5. J. S. Serafini, Bull. Am. Phys. Soc. 13, 1567 (1968).
6. A. R. Akhmedov and A. A. Zaitsev, Soviet Phys.-Tech. Phys. 8, 126 (1963).
7. N. D'Angelo and L. Enriques, Phys. Fluids 9, 2290 (1966).
8. J. S. Serafini, NASA TM X-1975 (1970).
9. A. Garscadden and K. G. Emeleus, Proc. Phys. Soc. 79, 535 (1962).
10. M. Sugawara and Y. Hatta, J. Phys. Soc. Japan 19, 1908 (1964).
11. A. Demetriades and E. Doughman, Phys. Fluids 8, 1001 (1965).
12. A. Demetriades and E. L. Doughman, AIAA J. 4, 451 (1966).
13. F. Klan, Zeit. fur Naturforschung 25, 263 (1970).
14. J. H. Malmberg, C. B. Wharton, and W. E. Drummond, in Proceedings of Second IAEA Conference on Plasma Physics and Controlled Nuclear Fusion Research (1965). Vol. 1, pp. 485-497.
15. J. A. Schmidt, Rev. Sci. Instr. 39, 1297 (1968).

16. D. E. Lencioni, J. W. Poukey, J. A. Schmidt, J. C. Sprott, and C. W. Erickson, Phys. Fluids 11, 1115 (1968).

17. J. R. Roth, D. C. Freeman, Jr., and D. A. Haid, Rev. Sci. Instr. 36, 1481 (1965).

18. J. R. Roth, Rev. Sci. Instr. 37, 1100 (1966).

19. J. R. Roth and M. Clark, Plasma Phys. 11, 131 (1969).

TABLE I

PLASMA CHARACTERISTIC	Low value	High value
Neutral number density	$1.5 \times 10^{12}/cm$	$2.5 \times 10^{12}/cm^3$
Electron number density	$5 \times 10^7/cm^3$	$5 \times 10^8/cm^3$
Electron kinetic temperature	8.3 eV	38 eV
Ion kinetic temperature	350.0 eV	930 eV
Plasma potential	+45 volts	+230 volts
Electron plasma frequency	64 MHz	202 MHz
Electron Gyro frequency	18 GHz	
Ion plasma frequency (D^+)	1.0 MHz	3.3 MHz
Ion gyro frequency (D^+)	5 MHz	
Debye distance	0.1 mm	6.5 mm
Langmuir probe roll-off frequency	2.7 MHz	5.5 MHz

TABLE II

	C_1	C_2	C_3
Shielded Langmuir probe	28 pF	84 pF	
Unshielded Langmuir probe	20 pF	84 pF	
Capacitive probe	22 pF	84 pF	0.4 pF

TABLE III

Response category	Number of runs	Percentage of total, %
Figure 10(a)	20	45.5
Figure 10(b)	15	34.0
Figure 10(c)	2	4.6
Figure 10(d)	6	13.6
Other	1	2.3
	44	100

TABLE CAPTIONS

Table I — Range of plasma characteristics at probe location. All runs were made with deuterium gas in a magnetic mirror configuration with a mirror ratio of 2.6:1, a maximum magnetic field of 1.0 T, and a magnetic field at the probe tip of 0.65 T.

Table II — Measured equivalent circuit parameters of the probes investigated.

Table III — The number of runs in each of five response categories illustrated in Fig. 10. These show the nature of the Langmuir probe response relative to that of the capacitive probe, while sampling the same volume of plasma

FIGURE CAPTIONS

(1) Cross sectional drawing of two of the four types of probes used in this investigation. (a) Shielded Langmuir probe. Note that the inner probe wire is coaxially shielded to within 6 mm of the end. The unshielded Langmuir probe is identical, but without the coaxial shield for a distance of 44 mm from the probe tip. (b) Ceramic covered capacitive probe. The pyrex covered capacitive probe was identical in all respects, but had a pyrex envelope instead of the ceramic one shown in the illustration.

(2) Equivalent circuits of both probes. Typical values are shown in Table II. The cable capacitance C_2 for both probes was high due to the unavoidably long separation of the probes from the cathode followers. The capacitance C_1 is the capacitance from the probe tip to ground, and C_3 from the capacitive probe tip to the plasma. R_s is the effective source resistance of the plasma. (a) Shielded Langmuir probe. (b) Capacitive probe.

(3) Theoretical frequency response for both probes. Note that ordinate is ratio of amplitudes, not dB. The solid line is that of the floating shielded Langmuir probe, from Eq. (1), given for several values of the source resistance. (b) The dotted line is the frequency response of the capacitive probe, as given by Eq. (2), for several values of the source resistance.

(4) Schematic diagram of instrumentation used for probes. The differential amplifier shown was not used in the differential mode for this investigation. The high pass filter was set at 150 kHz to avoid

overloading the spectrum analyzers. The Tektronix 1L5 was used over the frequency range 0.1 to 1.0 MHz, and the 1L10 unit over the range 1.0 to 10.0 MHz.

(5) Schematic of in situ calibration in vacuum tank with calibration cup. The inner plate of the calibration cup was driven with a constant amplitude signal from a variable frequency oscillator.

(6) Measured frequency response of capacitive and shielded Langmuir probes, using entire system without high-pass filter to cut off the large amplitude signal below 150 kHz. Note that, in the absence of plasma, the two probes had an essentially flat response over the frequency range from 0.2 to 10 MHz. (1) Capacitive probe. (2) Shielded Langmuir probe.

(7) Top view of experimental apparatus. The two probes under test are parallel and separated by 44 mm. The probe assembly is so mounted that a 180 degree rotation will interchange to the position of the two probes.

(8) Typical spectra measured by the two probes, corrected for small nonlinearities of the measuring system, and normalized to the amplitude at 1.0 MHz. System noise was subtracted off before plotting. (a) Ceramic capacitive probe. Note absence of signal at frequencies near 10 MHz. (b) Shielded Langmuir probe. Note rapid fall-off above 4 MHz, and noise picked up at high frequencies that is more intense than that detected by the capacitive probe.

(9) Ratio of response detected by shielded Langmuir probe to that of capacitive probe, normalized to unity at 1.0 MHz. Experimental error in this ratio was approximately $\pm 20\%$. Note relative fall-off of shielded

Langmuir probe response above 4 MHz, and the presence of more noise detected by the Langmuir probe at frequencies from 7.0 to 10.0 MHz, than was detected by the capacitive probe.

(10) Four types of relative probe characteristics most frequently observed when comparing the ceramic covered capacitive probe with the shielded Langmuir probe. (a) Fall-off of the Langmuir probe relative to the capacitive probe at about 4 MHz, without Langmuir probe noise at in the vicinity of 8.0 MHz. (b) Fall-off of the Langmuir probe relative to the capacitive probe at about 4 MHz, with presence of Langmuir probe noise at in the vicinity of 8.0 MHz. (c) Relative fall-off of Langmuir probe not apparent (at least in part because the signal of one or both probes disappeared in the noise below 4 MHz), but Langmuir probe noise was observed. (d) The signal of both probes disappeared in the noise at frequencies so low that neither the relative fall-off of the Langmuir probe nor the Langmuir probe noise at higher frequencies could be observed.

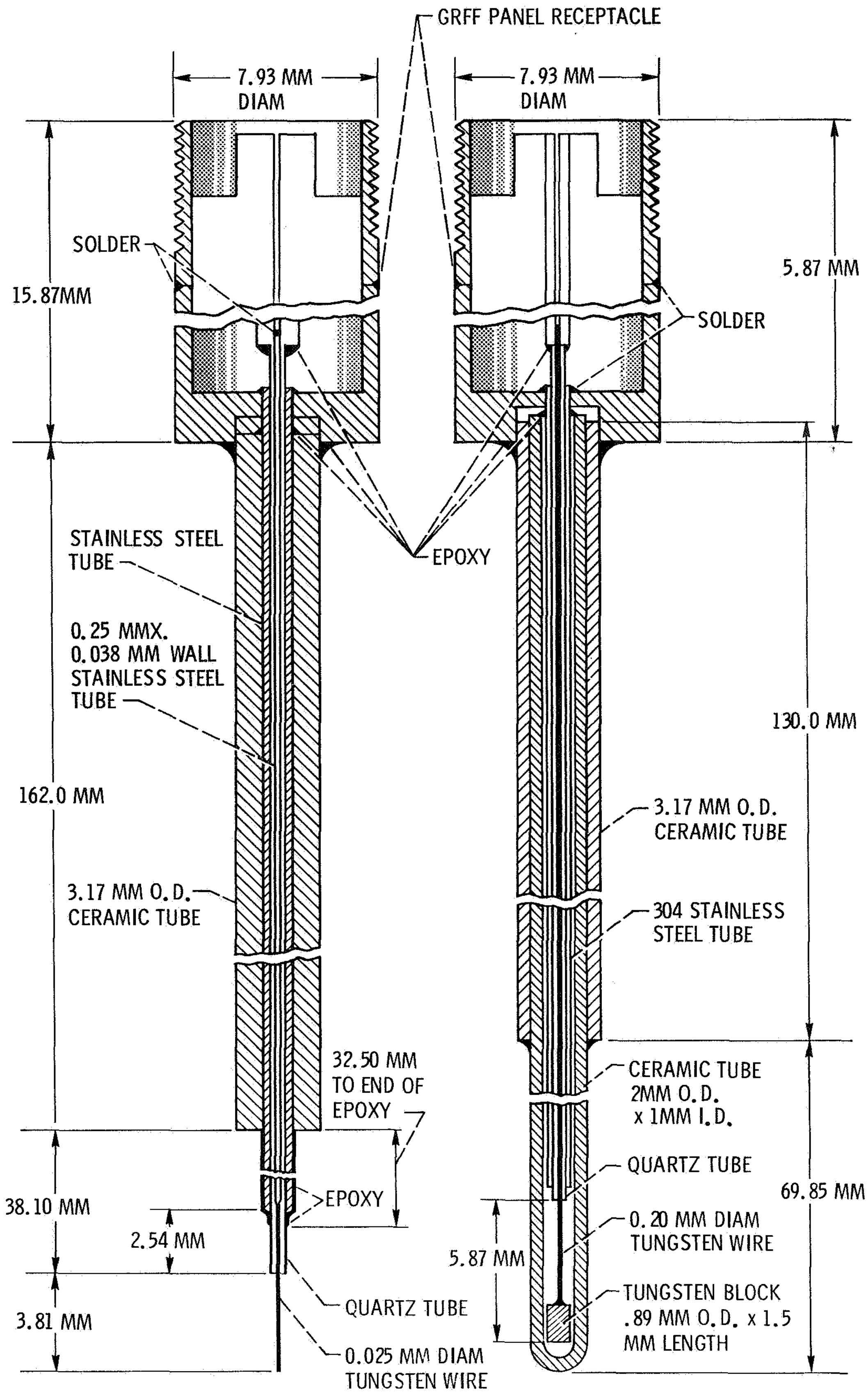

CD-10903-14

Figure 1.

CS-56435

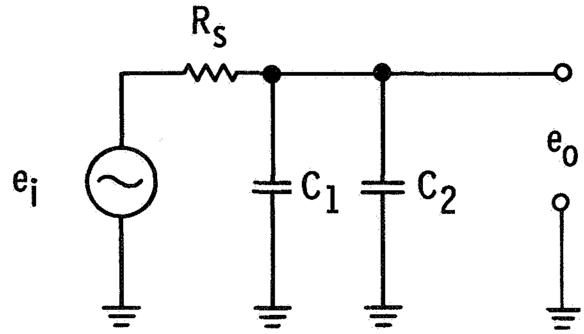

(A) LANGMUIR PROBE.

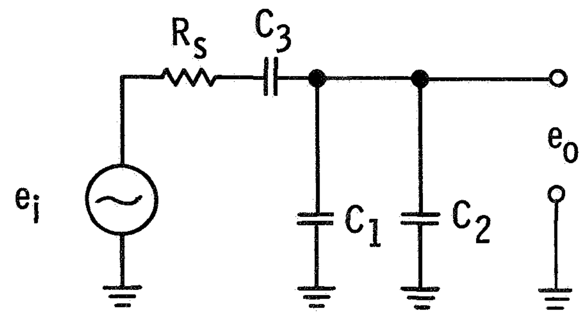

(B) CAPACITIVE PROBE.

Figure 2

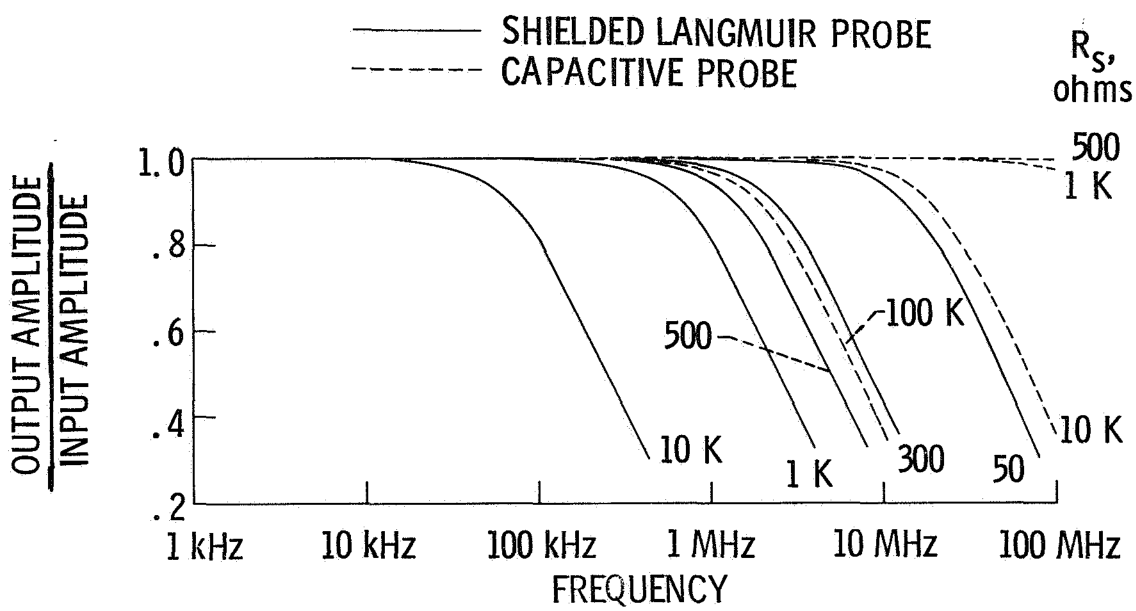

Figure 3

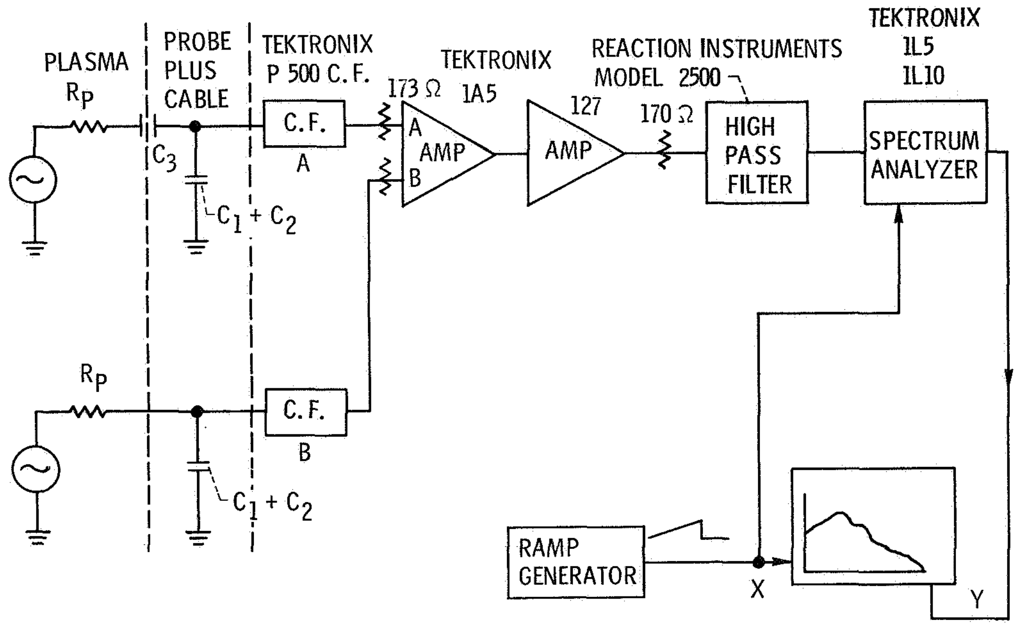

Figure 4

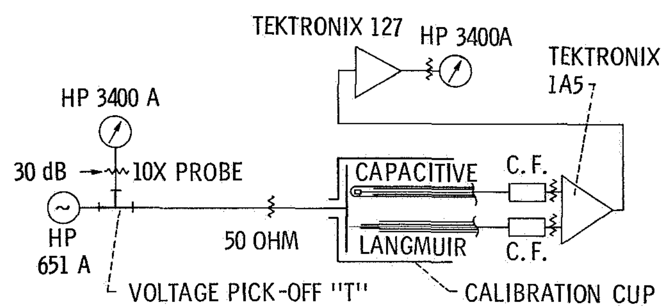

Figure 5

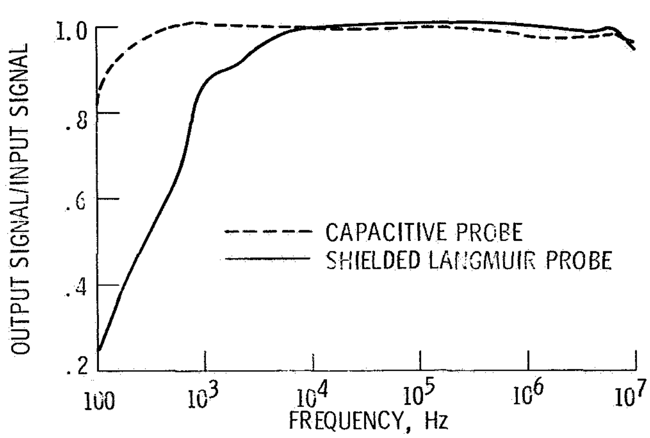

Figure 6

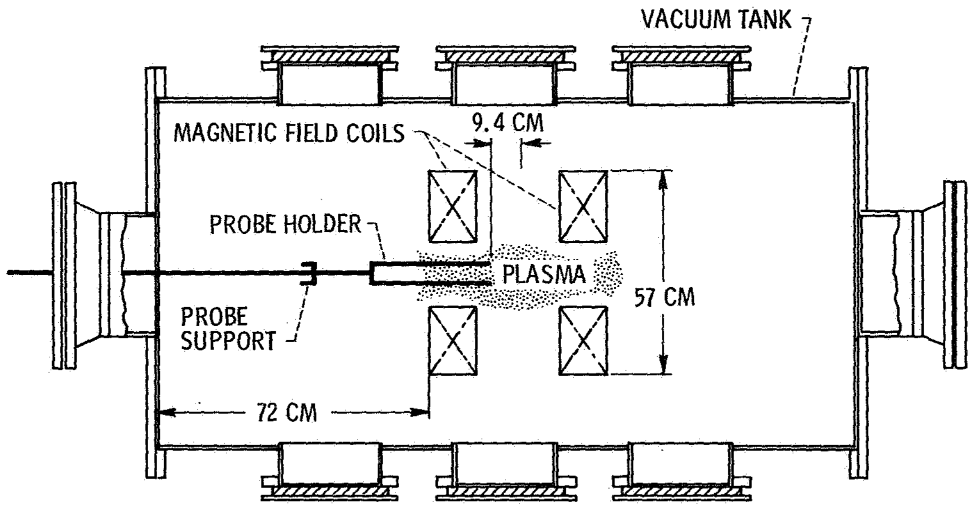

Figure 7

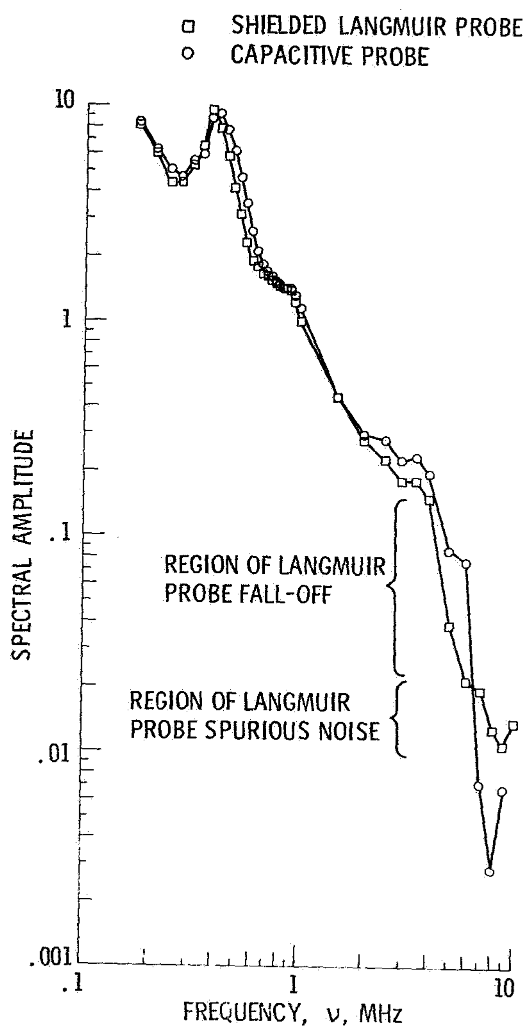

Figure 8

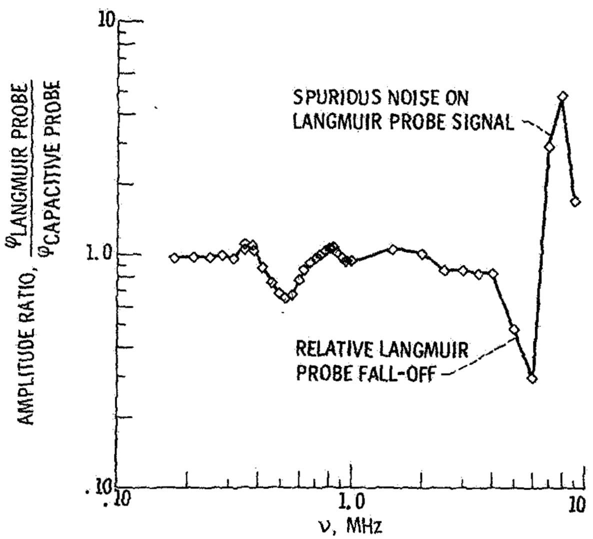

Figure 9

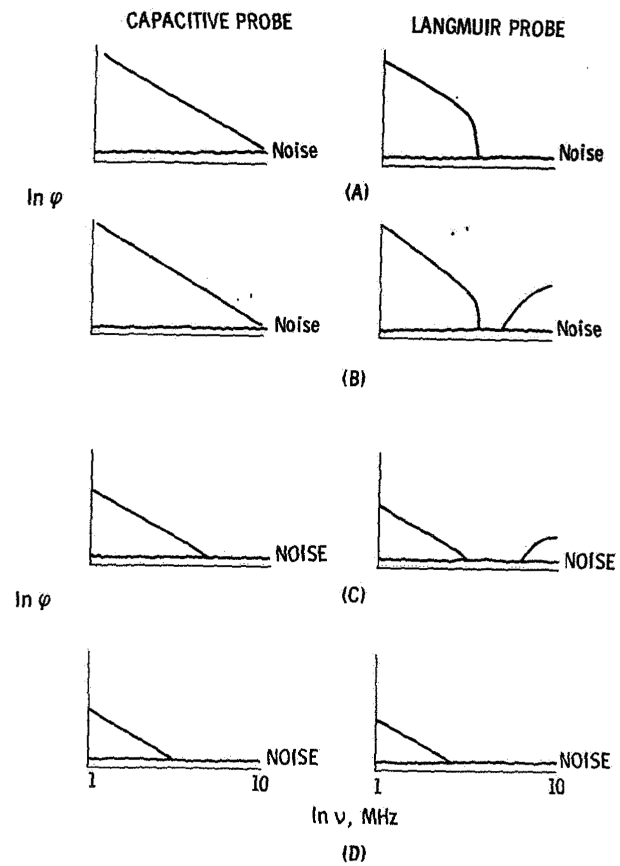

Figure 10. - Four types of relative probe characteristics most frequency observed.